Copyright © [2006] IEEE. Reprinted from

(Special Issue on Nonlocal, Collisionless Electron Transport in Plasmas - June 2006).

This material is posted here with permission of the IEEE. Internal or personal use of this material is permitted. However, permission to reprint/republish this material for advertising or promotional purposes or for creating new collective works for resale or redistribution must be obtained from the IEEE by writing to pubs-permissions@ieee.org.

By choosing to view this document, you agree to all provisions of the copyright laws protecting it.

Non-Local Effects in a Bounded Afterglow Plasma with Fast Electrons

Vladimir I. Demidov, Charles A. DeJoseph, Jr., and Anatoly A. Kudryavtsev *†

Abstract—Effects connected with non-locality of the electron energy distribution function (EEDF) in a bounded, afterglow plasma with fast electrons can lead to a significant (many times of T_e/e) increase in the near-wall potential drop, even if the density of this fast group is only a small fraction of the total electron density. This can substantially change the near-wall sheath thickness and electric field. Non-local fast electrons which are partially trapped in the plasma volume can increase the rate of stepwise excitation, supply additional heating to slow electrons and reduce their diffusion cooling rate. Altering the source terms of these fast electrons, to change their production rate will therefore alter the near-wall sheath and, through modification of the EEDF, a number of plasma parameters. Another possibility of modifying the EEDF is by application of a negative potential to a portion of the plasma boundary. This can allow modification of the fast part of the EEDF. The above effects and methods can be used in various research and technical applications.

Index Terms—Afterglow plasma, near-wall sheath, electron energy distribution function (EEDF), modeling, stepwise excitation, diffusion cooling.

I. INTRODUCTION

The plasma which exists in the discharge volume after termination or significant reduction of the sustaining electric field, is commonly referred to as the afterglow (or post-discharge) plasma [1]. In such a plasma (especially at low pressure), the electron temperature T_e relaxes to the atomic (ion) temperature (typically ~ 0.1 eV), due to electron-atomic collisions and diffusion cooling, much faster than the characteristic recombination time of the electrons. Due to this decreasing T_e, the number of electron-driven processes can be significantly reduced, despite a high electron density, which makes this type of plasma a convenient medium for measurements of rate constants and cross-sections of some plasma reactions [2–4]. The afterglow plasma exists in all pulsed plasma sources, which are now widely used in technical applications, and therefore, its investigation is important for optimization and development of various plasma systems [1, 5]. A similar plasma exists in flowing-gas systems, downstream of the discharge, which is commonly referred to as a flowing afterglow plasma [6], and far from the primary ionization source in non-homogeneous discharges. Properties similar to afterglow plasmas can be also found in non-electric excited plasmas, such as photoplasmas, created by external light.

Due to its practical importance, the afterglow plasma has been studied in great detail [1]. In particular, a number of plasma models have been applied to the afterglow regime. Fluid models (also referred to as the continuum models) have been widely used for simulations of afterglow plasmas (e.g., [7, 8]). The so-called global (volume-averaged) models of high-density, low-pressure discharges for time-varying excitation have recently been proposed by Lieberman and co-workers [9]. In both the fluid and global models, an ad hoc assumption of a Maxwellian electron energy distribution function (EEDF) is made. There are also a number of models with a volume-averaged kinetic treatment in order to predict zero-dimensional EEDFs in the local approximation (e.g., [10–12]. These models take into account various mechanisms leading to electron energy relaxation due to electron-atom collisions. A model with a self-consistent kinetic description of a low-pressure afterglow plasma was developed in [13, 14]. It was shown that the electron kinetics are essentially non-local and so knowledge of the spatial (and temporal) evolution of the EEDF is of vital importance.

With decreasing electron density, the frequency of electron-electron collisions, at an energy corresponding to the wall potential $\nu_{ee}(e\Phi_w)$, becomes less than the reciprocal of the ambipolar diffusion time for ions to the wall τ_a^{-1}. When this occurs, the EEDF "cutoff" effect was predicted in [14]. Under these conditions, the wall potential has to start decreasing fast enough spatially in order to let electrons leave the potential well and escape quickly to the wall. Such a rapid decrease in Φ_w must occur so that a part of the EEDF with energies close to $e\Phi_w$ can be effectively cut off from the bulk EEDF, which represents the "cutoff" mechanism. The particle

---

*Manuscript received August 2, 2005. This work was supported by The Air Force Office of Scientific Research. Copyright ©2006 IEEE. Reprinted from Special Issue on Nonlocal, Collisionless Electron Transport in Plasmas - June 2006. This material is posted here with permission of the IEEE. Internal or personal use of this material is permitted. However, permission to reprint/republish this material for advertising or promotional purposes or for creating new collective works for resale or redistribution must be obtained from the IEEE by writing to pubs-permissions@ieee.org. By choosing to view this document, you agree to all provisions of the copyright laws protecting it.

†V. I. Demidov is with UES, INC., 4401 Dayton-Xenia Rd., Dayton, OH 45432. C. A. DeJoseph, Jr. is with Air Force Research Laboratory, Wright-Patterson AFB, Dayton, OH 45433. A. A. Kudryavtsev is with Institute of Physics, St. Petersburg State University, St. Petersburg 198904, Russia.

loss due to the cutoff mechanism is accompanied by an energy loss which can be referred to as a modified form of diffusion cooling and it is the most important cooling process at low pressures. This effect was experimentally confirmed in [15].

Thus, the results of the direct comparison between the fluid and kinetic approaches imply that the fluid approach is physically inappropriate for describing a low-pressure afterglow plasma. Specifically, the fluid approach fails to predict correctly both the spatial and temporal evolution of the electron temperature [13]. Moreover, it has also been demonstrated in [13] that the use of the volume averaged (zero-dimensional) kinetic models may lead to erroneous results in simulating such a plasma. The non-local approach is most important over lengths which are less than the electron energy relaxation length λ_ε. At low pressure, when the plasma scale L is less than λ_ε, the EEDF is essentially non-local (see [16] for details), and the EEDF tail is depleted due to electrons escaping to the wall throughout the whole plasma volume. For atomic gases in the energy range $\varepsilon < \varepsilon^*$, where ε^* is the threshold energy for inelastic processes, where most electrons are concentrated, length $\lambda_\varepsilon = \lambda_e\sqrt{M/m} > 100\lambda_e$, where λ_e is the electron mean free path. Therefore the inequality $\lambda_\varepsilon >> L$ holds up to relatively high pressures of $pL < 10\,\mathrm{cm}\times\mathrm{Torr}$. This means, for instance, that for atmospheric pressure micro-discharges [17] (say, with characteristic dimension of 50 μm) these effects are very important over the whole plasma volume.

In this paper we discuss effects connected with non-locality of the EEDF in the afterglow plasma *with fast electrons* [18, 19]. We define the fast electrons as electrons which have energies ε_{ef} much higher than T_e, but usually less than ε^* (recall that the typical electron temperature in an afterglow is 0.1 eV). In the next section we discuss production mechanisms and the importance of fast electrons in the afterglow. Following that, in Sec. III we demonstrate the influence of fast electrons on the ambipolar electric field and wall potential. Sec. IV describes the influence of non-local effects on sheath properties. In Sec. V we illustrate the influence of these effects on the EEDF. Sec. VI deals with modification of the EEDF and in the last section we discuss possible application of these effects in research and applications and present some conclusions.

II. WHY FAST ELECTRONS ARE SO IMPORTANT IN AN AFTERGLOW PLASMA

Sources of fast electrons exist in many types of afterglow plasmas. Fast electrons can be injected from outside (for instance, electron beams) or can arise in the plasma volume as a result of various plasma-chemical reactions involving the participation of long-living excited states of atoms and molecules, negative ions, or photons from an external source. The density of excited atoms and molecules in the plasma can exceed by an order of magnitude the charged particle density and, as a result, the potential energy stored in excited states can surpass by many times the kinetic energy of the electron gas. Due to this large chemical activity of the excited states, their effective participation in ionization, dissociation and excitation should be taken into account. Examples of such processes are a number of reactions involving metastable states of atoms (A^*) or molecules, such as Penning ionization

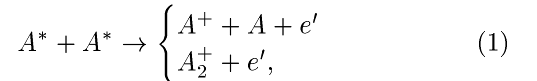

$$A^* + A^* \to \begin{cases} A^+ + A + e' \\ A_2^+ + e', \end{cases} \tag{1}$$

superelastic collisions

$$A^* + e \to A + e' \tag{2}$$

and monochromatic photon ionization from external light sources

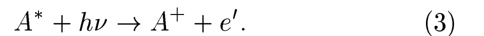

$$A^* + h\nu \to A^+ + e'. \tag{3}$$

In electronegative gases fast electrons can also arise in associative detachment reactions

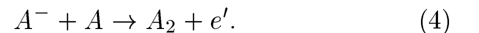

$$A^- + A \to A_2 + e'. \tag{4}$$

Here, A^+, A^-, and A_2^+ correspond to positive and negative atomic ions and molecular ions, and e' is a fast electron.

The energy of these fast electrons depends on the specific atom or molecule involved and for noble gases in reactions (1) and (2) are given in Table 1 [19]. Note that the width of the energy spectra of these fast electrons is much smaller than ε_{ef} and in many cases it can be taken as δ-function [20, 21]. For reaction (4) energies are, typically, not as large but can still be substantially greater than T_e. For example, for O_2 fast electrons have an energy of 3.6 eV.

The density of fast electrons, N_{ef}, is usually much smaller than the density of slow, bulk electrons N_{eb}. As a result, in many cases these fast electrons can not significantly change the average energy of all electrons ($\varepsilon_{ef}N_{ef} \ll T_eN_{eb}$) in the plasma. This case will be discussed below. If the density of fast electrons is so small that it cannot significantly effect the average electron energy, then why are they important? Under non-local conditions, this is because the electron current to

TABLE I: Energies of fast electrons ε_{ef} [in eV], arising in reactions (1) and (2).

Gas	He	Ne	Ar	Kr	Xe
ε_{ef}, reaction (1)	14.4	11.0	7.3	6.0	4.4
ε_{ef}, reaction (2)	19.8	16.6	11.5	9.9	8.3

the negatively biased plasma walls is transported only by the high energy part of electron population. For a Maxwellian EEDF the ratio of the density of trapped electrons which can not reach the wall to the density of free electrons which can reach walls is greater than 10^3. Since the number of free electrons is always small, the addition of even a small number of fast electrons with energies $\varepsilon_f >> T_e$ can dramatically change the characteristics of the plasma with a non-local EEDF. This explains why fast electrons can be so especially important in a non-local afterglow plasma. Note that to get similar effects in the fluid approach the fast electrons must significantly change the average electron energy, which requires a much higher N_{ef} (see, for example, [22]).

III. HOW DOES THE AMBIPOLAR ELECTRIC FIELD AND WALL POTENTIAL DEPEND ON THE PRESENCE OF FAST ELECTRONS?

Consider the ambipolar diffusion of charged particles in a low temperature plasmas with fast electrons. The ion and electron fluxes are given by the expressions

$$j_i = N_i u_i = -D_i \nabla N_i + b_i E_a N_i \tag{5}$$

and

$$j_e = N_{eb} u_{eb} = (-D_{eb} \nabla N_{eb} + b_{eb} E_a N_{eb}) \tag{6}$$

$$+(-D_{ef} \nabla N_{ef} + b_{ef} E_a N_{ef}).$$

Here N_i is the ion density, u the drift velocity of corresponding particles, D and b are the coefficients of diffusion and mobility, and E_a is the ambipolar electric field. The index i refers to the ions, e refers to the electrons, eb refers to the bulk plasma electrons, and ef refers to the additional group of fast electrons. As $D_e >> D_i$ and $b_e >> b_i$, for the ambipolar electric field we have

$$E_a = -\frac{D_{eb} \nabla N_{eb} + D_{ef} \nabla N_{ef}}{b_{eb} N_{eb} + b_{ef} N_{ef}} \tag{7}$$

Using the Einstein relation ($D_j / \ b_j = T_j$) we obtain

$$D_{ef} \nabla N_{ef} / (D_{eb} \nabla N_{eb}) = \bar{\varepsilon}_{ef} N_{ef} / T_e N_{eb}. \tag{8}$$

As $T_e N_{eb} >> \bar{\varepsilon}_f N_{ef}$, the presence of fast electrons does not influence E_a and

$$E_a = -\frac{T_e \nabla N_{eb}}{e N_{eb}} \tag{9}$$

which coincides with the well-known ambipolar field for a Maxwellian EEDF. Therefore, the diffusion of slow electrons and ions in the plasma volume does not depend on the presence of fast electrons. On the other hand, the ambipolar electric field is too small to significantly effect the diffusion of fast electrons and, therefore, they are transported via free (not ambipolar) diffusion. As a result, fast and slow electrons can be treated as two independent groups and the ratio N_{ef}/N_{eb} may vary from point to point in the plasma. This is justification for Eq. (6).

The situation is quite different at the plasma wall. Here, even for the case $T_e N_{eb} >> \bar{\varepsilon}_f N_{ef}$, the wall potential can depend significantly on the presence of fast electrons. Consider an approximate analytical expression for the wall potential Φ_w. Due to quasi-neutrality of the plasma, for dielectric walls the sum of the ion current and electron current to the wall is equal to zero at each point on the wall (for a conducting surface, this holds for an integral over all surfaces). The zero current condition has the form

$$j_i + j_{eb} + j_{ef} = 0, \tag{10}$$

where j_i is the ion current density, j_{eb} is bulk electron current density and j_{ef} is the current density of fast electrons. The ion flux is formed in the quasi-neutral plasma and is referred as the ion saturation current. This flux corresponds to the sum of the diffusion and conductivity fluxes (5), and for uniform temperatures equals the ambipolar flux

$$j_i = -D_a \nabla N_i / N_i, \tag{11}$$

The normal to the boundary density gradient is to be calculated in the region where the plasma is quasi-neutral and collisional, but not too far from the wall in order to consider the particle fluxes as conserved. The electron flux to the wall is equal to

$$j_{eb} = j_{eT} \times \exp(-e\Phi_w / T_e), \tag{12}$$

where the electron chaotic flux $j_{eT} = eN_{eb}\sqrt{T_e/2\pi m}$. Using eqs. (10) and (12) we obtain

$$e\Phi_w = \Phi_{wa} - T_e \times \ln\left(\frac{j_i}{j_i - j_{ef}}\right), \tag{13}$$

where

$$\Phi_{wa} = -T_e \ln\left(\frac{L}{\lambda_i}\sqrt{\frac{T_i}{T_e + T_i}}\right) \tag{14}$$

is the wall potential for the Maxwellian EEDF without fast electrons, λ_i is the ion free path length and T_i is the ion temperature.

Therefore, two situations are possible [18, 23]. If the magnitude of the fast electron current to the wall is less than the ion current, the wall potential should be small enough to allow some of the slow electrons to reach the walls (a few T_e/e). In the opposite case, the wall potential has to repel part of the fast electron current and, therefore, should approach ε_f/e [18, 19, 23]. The transition between the two regimes should be very abrupt, as

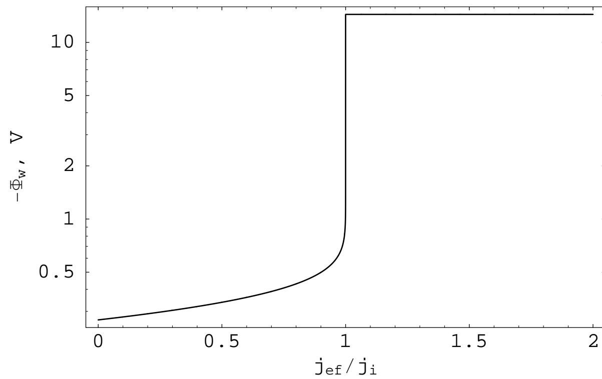

FIG. 1: Wall potential in helium afterglow plasma. $T_e = 0.1$ eV, $\varepsilon_{ef} = 14.4$ eV.

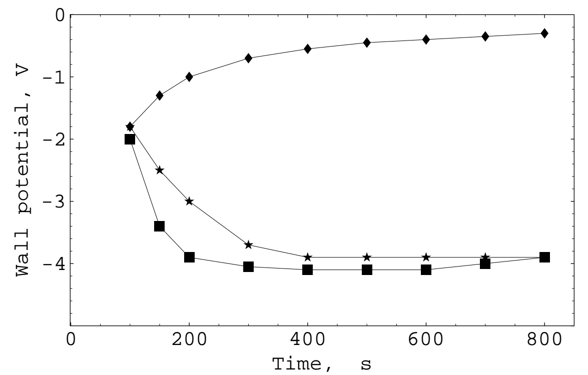

FIG. 2: Near-wall potential drop in Xe afterglow plasma. Measurements (stars), calculation with equation (13) (diamonds) and calculations taking into account fast electrons and arising of anomalous potential jump (boxes).

there are practically no electrons with energies between a few T_e and ε_f.

Thus, for the case $|j_{ef}| > j_i$, $e\Phi_w$ is close to the energy of the fast electrons. Since the electron spectra of reactions (1) and (2) have widths of a few tenths of an eV, and for the case $L \ll \lambda_\varepsilon$ this width does not change over the plasma volume, the wall potential deviates from ε_f/e by only a few tenths of a volt and one can neglect this deviation in the expression for the wall potential (13). As an example, fig. 1 illustrates the dependence of the wall potential on $|j_{ef}|/j_i$ obtained for the case of $\varepsilon_{ef} = 14.4$ eV (helium).

The ion flux to the wall can be determined directly from expression (11) or estimated by $j_i \approx SN_i/\tau_a$, (where S is the area of the plasma-limiting surface), which is adequate for most geometries, using the known T_e to calculate the characteristic time for ambipolar diffusion τ_a. Non-local fast electrons are produced in the volume by reactions (1-4) and are lost to the walls by free diffusion with characteristic time τ_{ef}. As $\tau_{ef} \ll \tau_a$, the non-local EEDF of the fast electrons is a narrow peak at the energy of their origin. The density N_{ef} can be estimated as

$$N_{ef} = I_{ef}\tau_{ef} \qquad (15)$$

and it is usually much less than the density of slow, Maxwellian electrons N_{eb}. For example, for the reaction of superelastic collisions (2), $N_{ef}/N_{eb} \sim N_m/N_a \sim 10^{-5}$. Here, N_m and N_a are the densities of metastable and ground state atoms. The flux of fast electrons to the plasma boundary can be found via their creation term from the equation

$$j_{ef} = \int\limits_V \sum I_j dV/S \qquad (16)$$

Since the intensity of the source I_j can, in many cases, be calculated for a given reaction, the flux j_{ef} can be found. For example, for reaction (1), $I_m = \beta_m N_m^2$, where β_m is the rate of (1).

Experimental confirmation of the above speculation has been conducted in Refs. [18, 24]. Two of the above conditions (Φ_w is a few T_e/e and Φ_w is close to ε_{ef}) can be realized in the process of plasma decay in the non-local regime: first, $j_{ef} < j_i$ during the initial time period; second, $j_{ef} > j_i$, in successive periods, when the bulk electrons cool to low temperatures. Fig. 2 shows the results of Φ_w measurements in a xenon afterglow at a gas pressure of $p = 0.2$ Torr, dc current in the pulse $i = 5$ mA, pulse duration 80 μs, and a repetition rate of 1 kHz in a glass tube of radius $R = 1.75$ cm [24, 25]. A molybdenum ring was inserted into a section of the tube which allowed measurements of the wall potential. A probe in the vicinity of the wall allowed measurements of the plasma potential (a second derivative method was used [26]). It could be clearly seen that a transition from a free diffusion regime ($j_{ef} < j_i$) to a regime with an anomalous large wall potential ($j_{ef} > j_i$) occured over a course of time in the afterglow (sometime between 100 and 200 μs of the afterglow). Calculations using equation (14) are not valid in this case. At the same time calculations which take into account fast electrons are in good agreement with experiment. Note, that for this case equation (13) can be used for times greater than 200 μs in the afterglow ($T_e << \varepsilon_{ef}$). For the transitional period (100-200 μs), the electron temperature is too high, for equation (13) to be used and one needs to calculate the EEDF using a more general approach such as in Ref. [13]. As a result, the sharp transition between the two regimes, predicted by eq. (13), is not observed in Fig 2.

IV. THE NEAR-WALL SHEATH DEPENDS STRONGLY ON ATOMIC AND MOLECULAR PROCESSES

Changing Φ_w leads to a change in the near-wall sheath properties. Generally, the presence of fast electrons should be taken into account for calculations of sheath thickness, potential, electron and ion densities in the plasma, presheath and sheath. However, as we assume

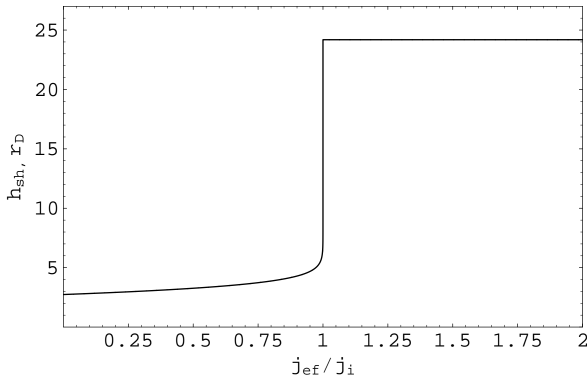

FIG. 3: The thickness of the near-wall sheath (in r_D units) calculated for argon afterglow plasma. $T_e = 0.1$ eV, $\varepsilon_{ef} = 7.3$ eV.

that $\varepsilon_{ef}N_{ef} \ll N_sT_e$, then in the quasi-neutral plasma and presheath, the density of fast electrons is negligible and need not taken into account. Therefore, analysis of the plasma and presheath may be done as in Ref. [27] in a plasma with a Maxwellian EEDF. In this situation the Bohm criterion will be the same as in a plasma without fast electrons (i.e. plasma with a Maxwellian EEDF with electron temperature T_e). Under conditions of low Φ_w, the sheath region can also be modeled without taking into account fast electrons in the sheath volume (density of fast electrons is negligible compared to density of bulk electrons). In this case fast electrons can only cause a small change in the wall potential. For large Φ_w, the density of bulk electrons in the sheath becomes very small with respect to the density of fast electrons and the latter should be taken into account. This means that in this region one cannot use the simple Boltzmann relationship for electron density and should use non-local plasma kinetics. Note also that in this case, despite a high Φ_w, the sheath is not completely unipolar due to the presence of fast electrons (compare with Ref. [28]). We can also conclude that during the transition between the two regimes, the sheath thickness changes from a thin sheath (a few Debye lengths, r_D) to a thick sheath (a few tens of r_D).

As an example, Fig. 3 shows the calculated near-wall sheath thickness h_{sh} in an argon post-discharge afterglow with an electron temperature $T_e = 0.1$ eV, which is typical for the afterglow. In these calculations only fast electrons arising from reaction (1) have been only taken into account. It can be seen that the transition between the two regimes (thin and thick sheath) occurs when $j_{ef} = j_i$ (which corresponds to n_f/n_b of order of 10^{-5}) and is very abrupt with respect to that ratio. Recall that this sharp rise is primarily the result of the absence of electrons within the energy interval from 0.5 to 7 eV. For these calculations we define the sheath sickness in accordance with refs. [29, 30] and use formulas of ref. [30]

$$h_{sh} = \left[\frac{\sqrt{2}}{3}(\sqrt{1-2\Delta V_{sh}/T_e}-2)^{3/2} + 2\sqrt{2}(\sqrt{1-2\Delta V_{sh}/T_e}-2)^{1/2}\right] r_D \tag{17}$$

for a collisionless sheath, neglecting the density of fast electrons in the sheath. Here, ΔV_{sh} is the potential drop in the sheath.

Thus, one finds that the wall potential and near-wall sheath can be changed significantly by the presence of fast electrons in the afterglow. At the same time the EEDF can also be changed. This will be discussed in the next section.

V. ELECTRON ENERGY DISTRIBUTION FUNCTION AND PLASMA PROPERTIES

As discussed in the previous sections, the wall potential Φ_w can be either a few T_e/e or close to ε_{ef}. In the first case the potential cannot affect the movement of fast electrons and they have free diffusion to the walls. In the second case only a portion of the fast electron flux, corresponding to j_i has free diffusion in the plasma volume, but the remaining portion, corresponding to $j_{ef} - j_i$ will be reflected by the wall potential. Reflection of a portion of the fast electrons back into the volume leads to a modification the high energy part of the EEDF. In Fig. 4 the calculated EEDF (full curve) and the experimental EEDF (dashed curve), obtained in a helium afterglow plasma at 1 Torr, in a glass tube 3.6 cm in diameter, are shown ($T_e = 1400$ K, $N_{eb} = 10^{11}$ cm^{-3}, and metastable density $N_m = 4.4 \times 10^{11}$ cm^{-3}). In this case $j_{ef}/j_i = 1.8$ and $\Phi_w = 12$ V. Since the experimental curve is a convolution of the EEDF with the instrument function, Fig. 4 also shows the convolution of the calculated EEDF with the instrument function (points). For comparison, the result of calculating the EEDF for the same conditions, but under the assumption of no trapped fast electrons ($j_{ef}/j_i < 1$) is also shown (dash-dotted curve). As can be seen, when the fast electrons are trapped, the high energy part of the EEDF (which is the part shown in Fig. 4) is markedly different from the case without trapped fast electrons. It has a continuous electron spectrum toward lower energies.

Changing the form of the EEDF can change a number of plasma properties. First of all, increasing the fast electron density can significantly increase the rate of stepwise excitation. It was shown in Ref. [31] that trapping these fast electrons can result in substantial light output, which is readily observed experimentally. At low pressures, radiation produced from recombination is negligible while that arising from stepwise excitation dominates the afterglow emission. These low-pressure effects have been experimentally investigated in a pulsed rf ICP discharge

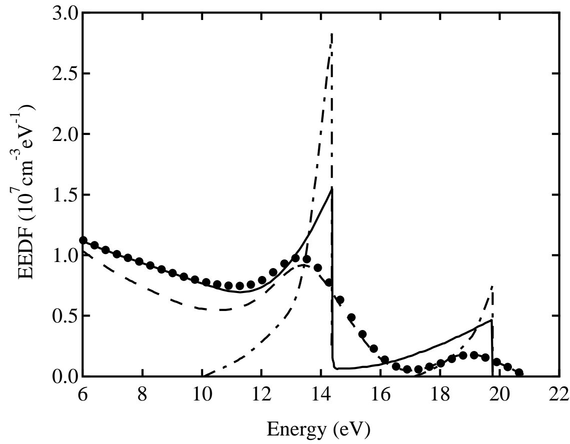

FIG. 4: Calculated and measured EEDF in a helium afterglow (1 Torr) with $\Phi_w = 12$V. See text for a description of the curves.

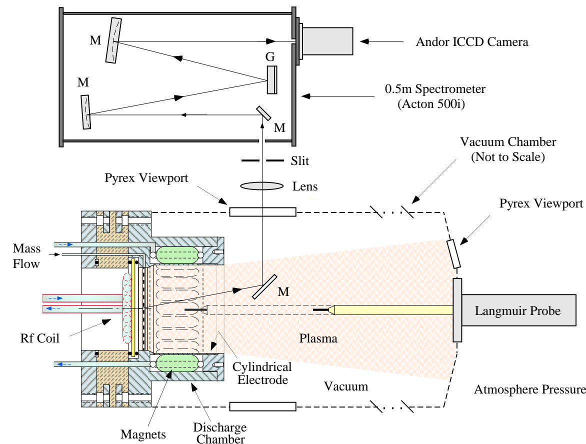

FIG. 5: Schematic diagram of the experimental set-up.

in Ar [32]. These experiments will now be discussed in detail.

The plasma excitation experiment has been described in [33]. A schematic of the experiment is shown in Fig. 5. The ICP system is a modified commercial ion-beam system built by Nordiko. Power of 13.56 MHz could be 100% modulated. Typical operating pressures range from 5 to 25 mTorr. The optical system includes an Acton 0.5 m spectrometer fitted with an Andor ICCD camera. A mirror, M, allows measurements of optical emission nearly parallel to the chambers axis. In Fig. 5, the discharge is formed in the “Discharge Chamber” near the rf coil and plasma can diffuse freely into the larger “Vacuum Chamber”. The length of the vacuum chamber is 1.22 m and radius is 40 cm. The length of discharge chamber is $L =$ 8 cm and radius is $R = 5.5$ cm.

Typical plasma density in the Discharge Chamber is between 10^{10} and 10^{12} cm^{-3}. Under these conditions the fast electron energy relaxation length in the afterglow is determined by the electron-atom elastic collisions, since

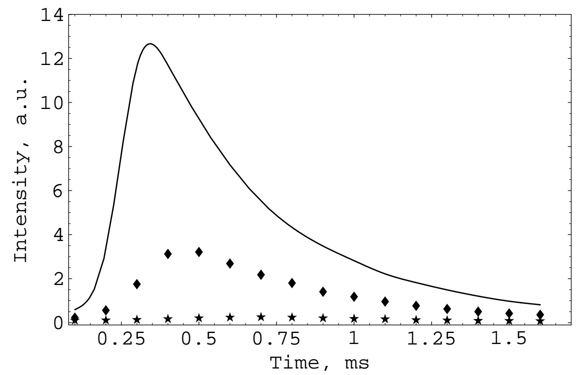

FIG. 6: Intensity of the Ar 420.1 nm spectral line after termination of rf pulse. Average power is 250 W and rf pulse duration is 300 μs. Gas pressure is 10 (stars), 15 (diamonds), and 20 mtorr (solid curve).

the region of high electron density is limited to the dimensions of the discharge chamber and therefore electron-electron collisions have little effect on λ_ε. In this case, for argon at a pressure 20 mTorr and an electron energy 7.3 eV, $\lambda_\varepsilon \approx 3.8$ m, which is much greater than largest dimension of the Vacuum Chamber. At the same time, $\lambda_e \approx 1.7$ cm. Additionally, at a pressure of 20 mTorr fast electrons loose less than 0.5 eV in collisions with atoms over a time of 200 μs. This means that for times of this order, fast electrons produced in reations (1) and (2) will have energy distributions with half-widths of not more than a few tenths of an eV.

The Langmuir probe allows us to conduct measurements of electron density N_e and temperature T_e. Unfortunately, this system does not have the sensitivity to measure the density of fast electrons arising in reactions (1) and (2) due to their small density [34]. It should be pointed out, however, that under higher pressure conditions in helium, Overzet [35] successfully used a similar probe system to measure the density of the fast group.

The transition between regimes of free-flight and partial trapping has been observed over a pressure range of 5 to 20 mTorr. During this transition, the wall potential increases from a few tenths of a volt to several volts. Also observed was a significant increase in the intensity of spectral lines corresponding to transitions between the argon $3p^5 4p$ and $3p^5 4s$ levels, which is consistent with stepwise excitation (see Fig.6). These experiments demonstrate the presence of self-trapping of fast electrons and the existence of large near-wall potentials in afterglow.

Another effect of partial trapping of fast electrons is seen as a change in the form the EEDF by the relaxation of fast electrons leading to heating of slow electrons. Due to this effect T_e can be significantly (a few times) higher than T_i even in far afterglow. This effect has been observed in Refs. [18]. A third effect is the absence of diffusion cooling for slow electrons, for the case $j_i < j_{ef}$ [23]. In the opposite case, diffusion cooling can still be

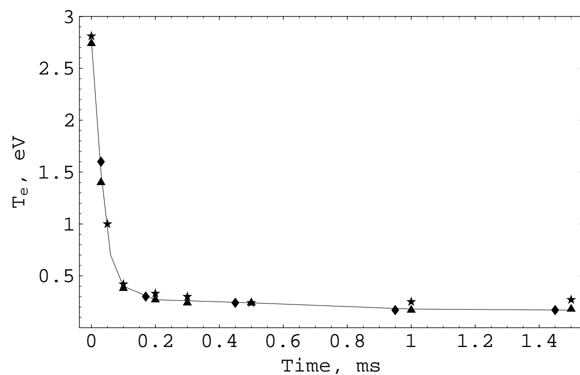

FIG. 7: Electron temperature after termination of rf pulse. Average power is 250 W and rf pulse duration is 300 μs. Gas pressure is 20 mtorr. Ring potential is -9 V: pure Ar (solid line), Ar with 0.6% of N_2 (triangles), Ar with 1.6% of N_2 (stars). Ring potential is 0 V: pure argon (diamonds).

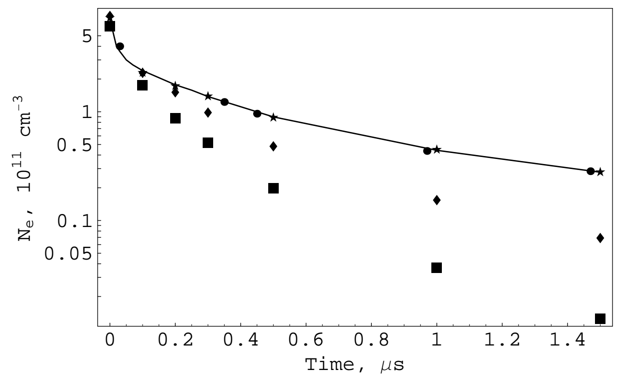

FIG. 8: Electron density after termination of rf pulse. Average power is 250 W and rf pulse duration is 300 μs. Gas pressure is 20 mtorr. Ring potential is -9 V: Pure Ar (solid line), Ar with 0.6% of N_2 flow (stars), Ar with 1.6% of N_2 flow (diamonds), and Ar with 3.2% of N_2 flow (boxes). Ring is grounded: Pure Ar (dots).

significantly reduced. This was investigated in Ref. [36].

VI. MODIFICATION OF THE ELECTRON ENERGY DISTRIBUTION FUNCTION

The existence of a non-local EEDF in the afterglow plasma allows for modification of different portions of the EEDF independently of each other. It was shown experimentally that the fast part of the EEDF can be changed independently of the slow part [37]. The experiments were conducted in the afterglow of a pulsed argon rf ICP discharge plasma in the device shown in Fig. 5. A cylindrical electrode (this is refered below as a "ring") with width 4 cm is located inside the discharge chamber, near its walls and close to the rf window. This electrode allows the plasma boundary potential to be changed over part of the discharge chamber. In these experiments, the presence of fast electrons has been detected from optical emission measurements. The data presented here is for the argon 420.1 nm emission line; however, all of the lines in the 400-900 nm range showed the same qualitative behavior. In the afterglow, emission from this line can only originate from collisions of electrons, with energy greater than 4 eV, with argon metastables. The intensity is therefore proportional to the product of the density of these species.

In the first series of experiments, the argon afterglow plasma was investigated for different potentials on the ring. The first results from this series showed that changing the ring potential between -15 and +10 V with respect to ground (walls of the Vacuum Chamber are grounded) had no measurable effect on the temporal behavior of N_e and T_e, as shown in Fig. 7 and Fig. 8. These data were taken on the axis of the Discharge Chamber at a distance of 6.5 cm from the rf window. In contrast, the temporal behavior of the argon emission line intensities depends strongly on the ring potential. Typical results

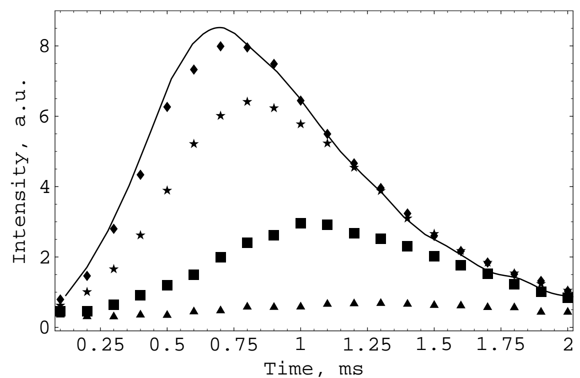

FIG. 9: Intensity of the Ar spectral line 420.1 nm after termination of rf pulse. Average power is 250 W and rf pulse duration is 300 μs. Argon pressure is 20 mtorr. Ring potential is -12 V (solid curve), -9 V (diamonds), -6 V (stars), -3 V (boxes) and 0 V (triangles).

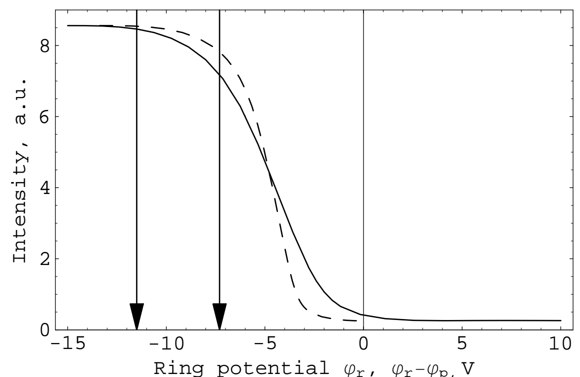

FIG. 10: Dependence of intensity of the Ar spectral line 420.1 nm for time 0.75 ms after termination of rf pulse on ring potential, φ_r (solid curve), and ring-plasma voltage, $\varphi_r - \varphi_p$ (dash curve). Voltage corresponding to energy of free electrons, arising in reactions (1), 7.3 eV, and to (2), 11.5 eV, are shown by arrows.

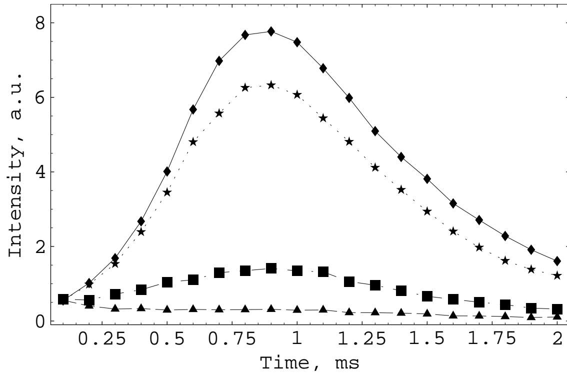

FIG. 11: Intensity of the Ar spectral line 420.1 nm after termination of rf pulse. Average power is 250 W and rf pulse duration is 300 μs. Gas pressure is 20 mtorr. Ring potential is -9 V. Pure Ar (diamonds), Ar with 0.3% of N_2 (stars), Ar with 0.6% of N_2 (boxes), and Ar with 1% of N_2 (triangles).

of the measurements are shown in Fig. 9 for the 420.1 nm line. Application of more negative potentials leads to a dramatic increase in emission intensity, which indicates a change in the density of the EEDF tail ($\varepsilon > 4$ eV) by more than a factor of 20 for the conditions shown in Fig. 9. This behavior can also be seen in Fig. 10, which shows the dependence of the line intensity on the ring potential (solid curve) at a fixed time of 0.75 ms after termination of the rf pulse (close to the intensity maximum). Changing of ring potential, as in figures 9 and 10, also changes the plasma potential. Therefore, in Fig. 10 the dashed line shows the dependence of the intensity on voltage between the ring and the central part of plasma. As can be clearly seen, the intensity increases sharply for potentials from -4 to -7 V with a much smaller change for more negative potentials. Again, this indicates a change in density of electrons with energies greater than 4 eV and demonstrates that this part of the EEDF can be readily moidified. An interesting point is that after 20-25 hours of operation, the ring becomes coated with a thin film of ceramic (presumably from the rf window) and the intensity no longer changes with ring potential. Polishing the ring returns the system to the state characterized by figures 4 and 5. These experiments demonstrate that the tail of EEDF can be modified without measurably altering N_e and T_e.

A second series of experiments was undertaken to demonstrates how modifying the source terms for fast electrons changes the EEDF. It was first determined that adding a small amount of nitrogen (up to 0.6% of flow) does not change the temporal behavior of N_e and T_e (see, Fig. 7 and 8). A further increase in flow leads to a slight increase in T_e and a decrease in N_e (increased decay rate of N_e and decreased ion production in the afterglow). The light emission during the rf pulse, while not shown, did not measurably change with up to 3.2% nitrogen flow. In contrast, fig. 11 shows the behavior of the 420.1 line as a function of nitrogen in the flow and shows a dramatic change with nitrogen concentration. Nitrogen is known to be an effective quencher of Ar^* [38] (leading to N_2(C-B) emission, which we observe in the afterglow) and thus reduces the production of fast electrons. If the fast electron density goes as $(Ar^*)^2$ (as in reaction (1)) and the emission goes as $Ar^* * e'$, then one expects the emission to go as $(Ar^*)^3$ and therefore depend strongly on the metstable density in the afterglow.

VII. CONCLUSIONS

Effects, described in this review, can be used for solving various fundamental problems of physics of plasmas, spectroscopy, etc. Regulation of the near-wall sheath can be useful for surface treatment and nano-fabrication. As an example of a fundamental application, we discuss here the unique possibility of reliable measurements of relative optical cross-sections for electron impact excitation from metastable states. These measurements are difficult to perform by other means. This problem has attracted significant attention in recent years (see, for example, refs. [43, 44]). The measurements can be performed in the device, shown in Fig. 5. As previously discussed, in the afterglow of a low-pressure rf ICP discharge, a plasma exists with a bimodal energy distribution. This consist of a large group with low electron temperature (~ 0.1 eV) and a much smaller group ($\sim 10^{-5}$) consisting of a narrow electron peak (width ~ 0.5 eV) at energies of a several eV which can exist for a few hundred microseconds. Therefore, for electron impact excitation from metastable states to levels with thresholds large enough to avoid excitation by slow electrons (of order of 1 eV), the intensity of a spectral line is proportional to corresponding cross-section.

As an example, we measured the ratio of the intensities of the Ar emission lines at 420.1 and 419.8 nm. in the afterglow. These lines originate from $3p_9$ and $3p_5$ (Paschen notation) levels in Ar. The ratio of $I_{420.1}/I_{419.8}$ should equal the ratio of the apparent cross-sections for stepwise excitation from the Ar $1s_5$ metastable level by electrons at 7.3 eV. The measurements were made at a gas pressure 20 mTorr. It was found that this ratio is equal to 3.8 ± 0.1 and relatively constant in the afterglow. Note that these two lines are very convenient for spectroscopic measurements due to their close proximity to one another, which usually does not require correction for the sensitivity of the detection system. This large ratio is not seen in the early stages of the rf pulse but is seen to increase as the discharge loads. This loading has previously been shown to correspond to the rapid build-up of metastables in the discharge [23]. This leads us to speculate that this ratio may be a sensitive indicator of the metastable density in the discharge.

VIII. ACKNOWLEDGEMENT

The authors are grateful to Allen Tolson for skillful technical assistance. This work was supported by the Air Force Office of Scientific Research.

[1] M. A. Lieberman and A. J. Lichtenberg, *Principles of Plasma Discharge and Material Processing.* New York: Wiley, 2005.

[2] V. A. Ivanov, "Dissociative recombination of molecular ions in noble-gas plasmas", Sov. Phys.-Usp., vol. 35, pp. 17-36, 1992.

[3] A. N. Klyucharev, "Chemi-ionization processes", Phys.-Usp., vol. 36, pp. 486-512, 1993.

[4] N. B. Kolokolov and A. B. Blagoev, "Ionization and quenching of excited atoms with production of fast electrons", Phys.-Usp., vol. 36, pp. 152-170, 1993.

[5] F. F. Chen, and J. P. Chang, *"Lecture Notes on Principles of Plasma Processing"*. New York: Kluwer/Plenum, 2002.

[6] D. Smith and P. Spanel, "Studies of electron-attachment at thermal energies using the flowing afterglow langmuir probe technique", Adv. At. Mol. Opt. Phys., vol. 32, pp. 307-343, 1994.

[7] J. W. Poukey, J. B. Gerardo, and M. A. Gusinow, "Properties of an afterglow helium plasma", Phys. Rev., vol. 179, pp. 211-226, 1969.

[8] D. P. Lymberopoulos, V. I. Kolobov, and D. J. Economou, "", J. Vac. Sci. Technol. A, vol. 16, pp. 564-571, 1998.

[9] M. A. Lieberman and S. Ashida, "Global models of pulse-power-modulated high-density, low-presssure discharges", Plasma Sources Sci. Technol., vol. 5, pp.145-158, 1996.

[10] C. Gorse, M. Capitelli, M. Bacal, J. Bretagne, and A. Lagana, "Progress in the non-equilibrium vibrational kinetics of hydrogen in magnetic multicusp H^- ion sources", Chem. Phys. vol. 117, pp. 177-195, 1987.

[11] T. Brauer, S. Gortchakov, D. Loffhagen, S. Pfau and R. Winkler, "The temporal decay of the diffusion-determined afterglow plasma of the positive column", J. Phys. D: Appl. Phys., vol. 30, pp. 3223-3239, 1997.

[12] V. Guerra, P. A. Sa, and J.Loureiro, "Relaxation of the EEDF in the afterglow of N_2 microwave discharge including space-charge field effects", Phys. Rev. E, vol. 63, pp. 046404, 2001.

[13] R. R. Arslanbekov, and A. A. Kudryavtsev, "Modeling of nonlocal electron kinetics in a low-pressure afterglow plasma", Phys. Rev. E., vol. 58, pp. 7785-7798, 1998.

[14] R. R. Arslanbekov, A. A. Kudryavtsev, and L. D. Tsendin, "Electron-distribution-function cutoff mechanism in a low-pressure afterglow", Phys. Rev. E., vol. 64, pp. 016401(1-10), 2001.

[15] A. Maresca, K. Orlov, and U. Kortshagen, "Experimental study of diffusive cooling of electrons in a pulsed inductively coupled plasma", Phys. Rev. E, vol. 65, pp. 056405, 2002.

[16] L. D. Tsendin, "Electron kinetics in non-uniform glow discharge plasma", Plasma Sources Sci. Technol., vol. 4, pp. 200-211, 1995.

[17] R. M. Sankaranand K. P. Giapis, "High-pressure micro-discharges in etching and deposition applications", J. Phys. D: Appl. Phys., vol. 36, pp. 2914-2921, 2003.

[18] V. I. Demidov, and N. B. Kolokolov, "Electron energy distribution, electron temperature, and stepwise excitation in afterglow plasma", Phys. Lett. A, vol. 89, pp. 397-400, 1982.

[19] V. I. Demidov, C. A. DeJoseph, Jr., and A. A. Kudryavtsev, "Effect of vmetastable atoms on near-wall voltage drop in the afterglow of a noble-gas radio-frequency inductive coupled plasma", Phys. Plasmas, vol. 11, pp. 5350-5353, 2004.

[20] A. Z. Devdariani, V. I. Demidov, N. B. Kolokolov, and V. I. Rubtsov, "Electron spectra from slow collisions of excited noble gas atoms", Sov. Phys. JETP, vol. 57, pp. 960-964, 1983.

[21] A. B. Blagoev, N. B. Kolokolov N.B., and A. A. Kudrjavtsev, "Interaction processes with creation of fast electrons in the low temperature plasma", Physica Scripta, vol. 50, p.371-402, 1994.

[22] K. Sato and F. Miyawaki, "Formation of presheath and current-free double layer in a two-electron-temperature plasma", Phys. Fluids B, vol. 4, pp. 1247-1254, 1992.

[23] V. I. Demidov, and N. B. Kolokolov, "Electron energy distribution functions in an afterglow plasma. V. Charged-particle diffusion and the distribution function", Sov. Phys. Tech. Phys., vol. 25, pp. 338-343, 1980.

[24] V. I. Demidov, N. B. Kolokolov, and O. G. Toronov, "Electron energy distribution and potential drop near the wall in a plasma with fast-electron sources", Sov. J. Plasma Phys., vol. 12, pp. 402-405, 1986.

[25] C. A. DeJoseph, Jr., V. I. Demidov, and A. A. Kudryavtsev, "Anomalously high near-wall sheath potential drop in a plasma with non-local fast electrons", Phys. Rev. Lett., vol. 95, pp. 215002, 2005.

[26] V. I. Demidov, S. V. Ratynskaia, and K. Rypdal, "Electric probes for plasmas: the link between theory and instrument", Rev. Sci. Instrum., vol. 73, pp. 3409-3439, 2002.

[27] K.-U. Riemann, "The Bohm criterion and boundary conditions for amulticomponent sistems", IEEE Trans. Plasma Phys., vol. 23, pp.709-716, 1995.

[28] K.-U. Riemann, and L. Tsendin, "Unipolar ion sheath", J. Appl. Phys., vol. 90, pp. 5487-5490, 2001.

[29] R. N. Franklin, "The plasma-sheath boundary region", J. Phys. D: Appl. Phys., vol. 36, pp. R309-R320, 2003.

[30] A. Kono, "Structure of collisional and collisionless sheath: closed expressions for sheath thickness", J. Phys. D: Appl. Phys., vol. 37, pp. 1945-1953, 2004.

[31] V. I. Demidov, N. B. Kolokolov, "Study of elastic electron collisions by plasma electron spectroscopy", Sov. Phys. J., vol. 30, pp.97-99, 1987.

[32] C. A. DeJoseph, Jr., and V. I. Demidov, "Spectroscopic study of the pulsed argon rf ICP discharge: Stepwise excitation in the afterglow and its application in optical spectroscopy", J. Phys. B: At. Mol. Opt. Phys., vol. 38,

pp. 3805-3814 (2005).

[33] W. Guo, and C. A. DeJoseph, Jr., “Time-resolved current and voltage measurements on a pulsed rf inductively coupled plasma”, Plasma Sources Sci. Technol., vol. 10, pp. 43-51, 2001.

[34] C. A. DeJoseph, Jr., and V. I. Demidov, “Diode calibration of a Langmuir probe system for measurements of electron energy distribution functions in a plasma”, Rev. Sci. Instrim., vol. 76, pp. 086105, 2005.

[35] L. J. Overzet, and J. Kleber, “Effect of metastable atoms on the electron energy probability functions in afterglows”, Plasma Sources Sci. Technol., vol. 7, pp. 512-523, 1998.

[36] N. B. Kolokolov, A. A. Kudryavtsev, and O. G. Toronov, “Excited atoms and diffusion cooling of electrons in plasmas”, Sov. Phys. Tech. Phys., vol. 30, pp. 1128-1132, 1985.

[37] C. A. DeJoseph, Jr., V. I. Demidov, and A. A. Kudryavtsev, “Modification of a non-local electron energy distribution in a bounded plasma”, Phys. Rev. E, vol. 72, pp. 036410, 2005.

[38] D. H. Steadman, and D. W. Setser, “Chemical applications of metastable argon atoms II. A clean system for the formation of $N_2(A^{3\sigma+}{}_u)$”, Chem. Phys. Lett., vol. 2, pp. 542-544, 1968.

[39] V. I. Demidov, N. B. Kolokolov, A. P. Mezentsev and A. S. Mustafaev, “Electron velocity distribution and potential drop near the wall in the cathode plasma of an electric discharge”, Sov. J. Plasma Phys., vol. 12, pp. 866-868, 1986.

[40] M. A. Biondi, “Diffusion cooling of electrons in ionized gases”, Phys. Rev., vol. 93, pp. 1136-1140, 1954.

[41] A. K. Bhattacharya and J. H. Ingold, “Diffusion cooling of electrons in afterglow plasma”, J. Appl. Phys., vol. 43, pp. 1535-1542, 1972.

[42] D. Trunec, P. Spanel, and D. Smith, “Electron temperature relaxation in afterglow plasmas: diffusion cooling”, Contrib. Plasma Phys., vol. 34, pp. 69-79, 1994.

[43] R. O. Jung, T. E. Stone, J. B. Boffard, L. W. Anderson, and C. C. Lin, “Electron impact excitation out of metastable levels of kripton”, Phys. Rev. Lett. Vol. 94, pp. 163202, 2005.

[44] A. Dasgupta, K. Bartschat, D. Vaid, A. N. Grum-Grzhimailo, D. H. Madison, M. Blaha, and J. L. Giuliani, “Electron-impact excitation from the $4p^5 5s$ metastable states of kripton”, Phys. Rev. A, vol. 65, pp. 042724, 2002.